Embodied swarming based on back propagation through time shows water-crossing, hourglass and logic-gate behaviors

Yukio-Pegio Gunji[1, 5], Hisashi Murakami[1], Takayuki Niizato[1], Andrew Adamatzky[2], Yuta Nishiyama[1], Koichiro Enomoto[3], Masashi Toda[3], Toru Moriyama[4], Tetsuya Matsui[1] and Kojiro Iizuka[4]

[1]Kobe University, Department of Earth & Planetary Sciences, Kobe University, Kobe 657-8501, JAPAN, [2] University of the West England, Bristol, BS16 1QY, UK [3] Hakodate Future University, Hakodate 041-8655, JAPAN, and [4] Young Researchers Empowerment Project, Shinshu University, Ueda 386-8567, JAPAN

[5]Corresponding author: yukio@kobe-u.ac.jp

Abstract

A flock, school, and swarm are collective behaviors that can be compared to a human consciousness or body. Through recent developments in image analysis and model simulation, it has been found that the collective behavior of animals can, as a whole, show characteristics of a single "body". It has also been found that intrinsic noise can positively contribute to swarming and/or flocking. Motivated by field observations of soldier crabs, *Mictyris guinotae*, we propose a swarm model based on inherent noise and back propagation in time that mimics mutual anticipation. A swarm generated by this model is characterized by flexible, dynamical and robust behavior containing inherent turbulence. We demonstrate that the model can produce water-crossing, hourglass and logic gate behaviors, which are also found in real soldier crabs. We describe how a sense of ownership and a sense of agency of the "body" arise in our model, and we propose that the concept of a body should be verified in terms not of stability but of robustness.

Introduction

Does a swarm, flock or school have a single consciousness or body (Vicsek, 2001, Couzin, 2007; 2008; 2010, Sumpter, 2010)? This question has been addressed in the context of collective decision making by computer models, particularly BOIDS (Reynolds, 1987) and SPP (Vicsek et al., 1995, Czir´ok et al. 1996). Owing to developments in image analysis that have made it possible to obtain kinetic data on the movements of real organisms (Ballerini et al., 2008a, b, Carere et al., 2009), several internal dynamical structures within groups have recently been identified. These structures include topological distance (Ballerini et al., 2008b), scale free correlation (Cavagna et al., 2010) and inherent noise (Yates et al., 2009). This research also suggests that inherent turbulence could play an essential role in collective motion. The collective behaviors of animals might be based on inherent noise, and the internal structures of a group are perpetually generated and modified to maintain a robust unity as a whole.

A flexible but robust swarm (flock or school) can be compared to a human's body (Gunji et al., 2010). In this sense, an animal group might recognize external objects in the environment by an embodied cognitive process (Varela et al., 1992, Pheifer and Scheier, 2001, Pheifer et al., 2007). Human body awareness can be described by a sense of ownership (i.e., the sense that I am the one who is undergoing an experience) and of a sense of agency (the sense that we are the initiators of our actions) (Wegner et al., 2004, Tsakiris, et al., 2008). Although a body appears to be very stable and unambiguous, it is well known that synchronous visuo-tactile stimulus can make body illusions, such as the rubber hand illusion (Botvinick, M. and Cohen, 1998) and an out-of-body experience (Lenggenhager et al., 2007, Ehrsson, 2007) possible. The body is also a robust and flexible system that can be adapted to environments. The problem still remains whether a swarm, flock and school can be compared to a "body" in these senses.

Here, we show how inherent noise in conjunction with organisms' mutual anticipation can actively contribute to the generation and maintenance of a robust swarm in a computer model. Mutual anticipation was implemented by asynchronous updating and back propagation through time. The time slice of a swarm is thus so complex that a swarm is robustly maintained and contains inherent turbulence. The model was constructed through observations of soldier crabs, *Mictyris guinotae* (Bradshaw and Scoffin, 1999, Shih., 1995, Peter et al., 2010). Our model can reproduce a swarm entering and crossing water through the emergence of a highly concentrated subpopulation driven by inherent turbulence; an hourglass of crabs showing regular oscillations; and collision-based-computing logic gates implemented by a swarm ball. The generation of these behaviors depends on the robustness and flexibility of swarming. Finally, we argue that a body-like character is embedded in our swarm model in the form of the interplay between anticipation and memory.

Swarming by mutual anticipation

Through observations of soldier crabs in the Iriomote Islands, Okinawa Prefecture, Japan, we discovered a role for inherent turbulence in collective behavior. A swarm of soldier crabs always contains inherent turbulence such that individuals in a swarm have different velocities, while the swarm maintains a coherent and dense unity. Inherent

turbulence in particular plays an essential role in water-crossing behavior. When a small swarm of soldier crabs confronts a water front, it cannot enter the water and moves along the perimeter of the water pool. In moving along the water front, inherent turbulence creates a highly concentrated locus inside the swarm, which can then enter and cross the water.

If inherent turbulence provides the essential mechanism to generate robust collective behavior, an important question is whether this robustness can be distinguished from stability. In the context of stability, perturbations conflict with the mechanism that generates order. In the context of robustness, inherent noise positively contributes to the generation of collective behavior. To implement inherent noise, we proposed a mechanism of mutual anticipation based on multiple potential transitions.

Basic model

A model is defined in a discrete space of $S \times S$ with $S = \{1, 2, \ldots, s_{MAX}\}$. The co-ordinate of the k^{th} agent at the t^{th} step is given by

$$\boldsymbol{P}(k, t) = (x, y) \tag{1}$$

where $x \in S$, $y \in S$, and $k \in K=\{1, 2, \ldots, N\}$. Each k^{th} agent at the t^{th} step has P number of potential vectors $\boldsymbol{v}(k, t; i)$ with $i \in I = \{0, 1, \ldots, P\text{-}1\}$. If $i = 0$, the vector is $\boldsymbol{v}(k, t; 0)$, which is known as the principal vector. Otherwise, the vector is represented by the angle $\theta_{k,t}$, such that

$$\boldsymbol{v}(k, t; i) = (Int(L\eta_i \cos(\theta_{k,t}+\xi_i)), Int(L\eta_i \sin(\theta_{k,t}+\xi_i))) \tag{2}$$

where for any real number x, $Int(x)$ represents integer X such that $X \le x < X + 1$. L is the length of principal vector. Because of the wrapped boundary, X belongs to S. If $i \neq 0$, random values η_i and ξ_i are selected with equal probability from $[0, 1]$ and $[-\alpha\pi, \alpha\pi]$, respectively. The target of the vector is represented by $\tau(k, t; i) = \boldsymbol{P}(k, t) + \boldsymbol{v}(k, t; i)$.

The mutual anticipation depends on the popularity of a site,

$$\zeta(x, y; t) = \begin{cases} |\{\tau(k, t; i), k \in K, i \in I \mid \tau(k,t; i)=(x, y)\}|, \\ \quad \text{If } {}^{\forall}(k \in K)\boldsymbol{P}(k, t) \neq (x, y); \\ 0, \quad \text{otherwise.} \end{cases} \tag{3}$$

$\zeta(x, y; t)$ represents the number of potential transitions whose targets reach the site (x, y) where there is no agent. Before updating the location, for any (x, y) at the t^{th} step and $\omega(x, y; t) \in \{0, 1\}$ we set $\omega(x, y; t) = 0$.

The agents' locations are updated asynchronously. If there exists $i \in I$ such that $\zeta(\tau(k, t; i)) \ge 2$, the next site for the k^{th} agent is defined by

$$\boldsymbol{P}(k, t+1) = \tau(k, t; s), \tag{4}$$

where s satisfies the condition such that for any $i \in I$, $\zeta(\tau(k, t; s)) \ge \zeta(\tau(k, t; i))$. These conditions ensure that an agent moves to the most popular site. If multiple sites satisfy this condition, one is chosen randomly. Because the popularities are propagated backward in time, agents in a swarm can anticipate each other's moves.

A set of updated sites is represented by $U_N = \{(x, y) \in S \times S \mid \boldsymbol{P}(k, t+1) = (x, y)\}$. The vacated site generated by equation (4) is recorded in memory as $\omega(x, y; t) = 1$ if $\boldsymbol{P}(k, t) = (x, y)$ and $\boldsymbol{P}(k,t+1) \in U_N$. An agent that is not updated by equation (4) then moves to the vacated site by

$$\boldsymbol{P}(k, t+1) = Rd\{(x, y) \in N_f \mid \omega(x, y; t)=1\}, \tag{5}$$

if $|\{(x, y) \in N_f \mid \omega(x, y; t)=1\}| \ge 1$, where RdJ represents an element randomly chosen from set J, and N_f is the follower's neighborhood. The agent moving by eq-(5) is called a follower because it follows a predecessor.

If an agent is not updated by (4) or (5), it moves by

$$\boldsymbol{P}(k,t+1) = Rd\{\tau(k, t; i) \mid {}^{\forall}(j \in K')\boldsymbol{P}(j, t) \neq \tau(k, t; i) \wedge \tau(k, t; i) \notin U_N\} \tag{6}$$

where K' is an index set of agents that are not updated. An agent moving by eq-(6) is called a free mover.

Finally, principal vectors are locally matched with each other in the neighborhood through velocity matching, M. This matching operation is expressed as

$$\theta_{k,t+1} = \langle \theta_{k,t} \rangle_M. \tag{7}$$

The bracket with M represents the operation of averaging velocity directions in the neighborhood, M.

Fig. 1a shows the neighborhood of velocity matching and of the follower. Figure 1b shows the procedure of velocity matching, mutual anticipation, and following.

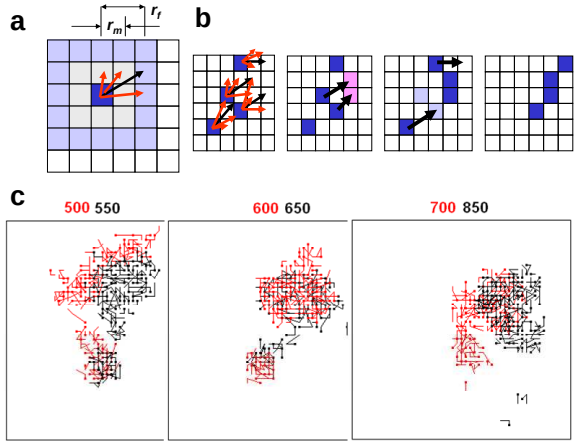

Figure 1 Schematic diagram of the transition and time development of the model simulation: (a) Principal vector (black arrow) and alternative vectors (red arrows) of a crab (blue square) in the matching neighborhood with radii r_m (pale gray lattices) and the following neighborhood with radii r_f (pale gray + pale blue lattices). (b) Transitions of crabs in a two-dimensional discrete space. Velocity matching (far left), mutual anticipation (second from left), following and free movement (second from right) and the resulting distribution at the next step (far right). (c) Time development (t = 500-850) of our swarm model of 100 agents, with $P = 20$, $\alpha = 0.9$, $L = 4$, $r_a = r_f = 2$.

First, velocity matching is applied to the principal vectors, and the agents then move to the most popular site (pink site in Fig. 1b), yielding a vacant site (pale blue site in Fig. 1b). Highly popular anticipated sites propagate backward in time, revealing the asynchronous transitions. Thus, mutual anticipation is here implemented by back propagation in time. Agents move to a vacant site if it is within the follower's neighborhood. Fig. 1c shows a series of snapshots of our swarm model. Each agent is represented with its 5-step trajectories. It is easy to see that a swarm contains turbulent motion despite maintaining a highly dense whole.

Fig. 2a shows polarization/density of a swarm plotted against external perturbation in our model with $P = 1$. Polarization is defined by the length of the average velocity over all agents in a swarm. Density is defined by the average number of agents in the neighborhood of 20×20 lattices. In the model with $P = 1$, the external perturbation, ξ, is randomly chosen from [0, 1] and is coupled with velocity matching. When the projected velocity of agent is expressed as (v_x, v_y), $v_x + \xi$ and $v_y + \xi$ are given for the unit vector. If $P = 1$, the model corresponds to BOIDS because each agent has only one velocity. The coherence of a swarm can result only from velocity matching or high polarization; the more polarized and dense the population, the less external perturbation there is.

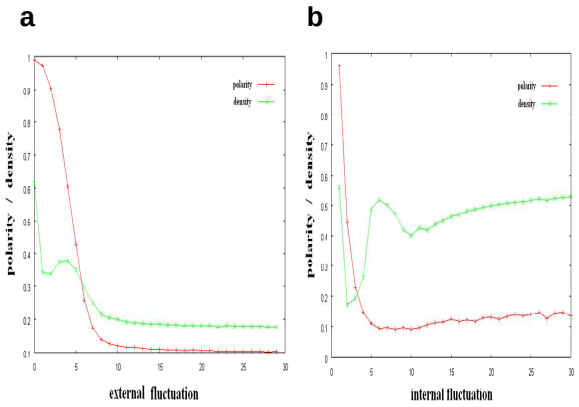

Figure 2 Polarization/density plotted against perturbation. (a) The polarization/density ratio plotted against external perturbation in the model with $P = 1$. (b) The ratio plotted against internal perturbation, which is defined as the number of potential transitions normalized by the maximum number of potential transitions. For this plot, P ranged from 1 to 30.

Fig. 2b shows the polarization/density of a swarm plotted against the inherent perturbation in our model. The inherent perturbation is expressed by $(P - 1)/P_{MAX}$, where P is given from 1 to P_{MAX} (30). The more inherent noise (i.e., more P) that is present, the higher the density and the lower the polarization are. This relationship reveals that a highly dense swarm is generated by mutual anticipation and/or inherent noise. For this reason, a coherent swarm (i.e., a highly dense swarm with an extrinsic boundary) contains inherent turbulence.

In the next section, we illustrate how inherent noise positively contributes to robust swarm behavior by demonstrating the role of noise in water-crossing behavior, hour glass behavior and collision-based computing implemented by swarm balls.

Water-crossing behavior

The water-crossing behavior observed in real soldier crabs can be easily approximated by our model. To introduce a tidal pool into the simulation, we define a specific area $U_p \subseteq S \times S$ in which the condition allowing mutual anticipation is replaced by

$$\zeta(\pi(k, t; i)) \geq c. \quad (8)$$

The value c is an integer larger than 2. Because $c > 2$, it is more difficult for agents to go through the area U_p. Only by introducing the specific area U_p can we simulate the behavior of crossing water.

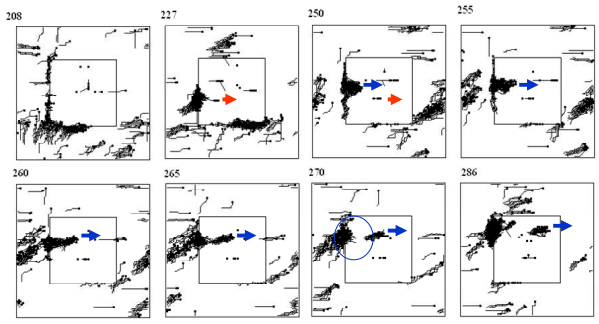

Figure 3 Snapshots of the time development of swarm trajectories in a model simulation. Numbers in the upper left of each plot denote the time step. Each agent is represented with its 5-step trajectories. The rectangle located in the center indicates U_p, which represents a tidal pool. For these simulations, $P = 10$, $\alpha = 0.3$, $L = 4$, and $r_a = r_f = 2$. Blue and red arrows represent the directions of motion of swarms. Blue circle represents highly concentrated area of a swarm.

Fig. 3 shows a series of snapshots of our swarm model demonstrating water-crossing behavior. Although a single agent or a small swarm cannot enter the tidal pool, a highly concentrated, large swarm can enter and cross the tidal pool. These behaviors are consistent with the behaviors of real soldier crabs observed in Iriomote islands.

Fig. 4 shows the frequency of a swarm invading the tidal pool in a model given by $P = 20$, $\alpha = 0.5$, $L = 4$, and $r_a = r_f = 2$. For each experiment, we prepared 2000 cases of a swarm confronting the tidal pool. If the size of a swarm exceeds a certain value, a constant high probability of invasion is achieved. If P is smaller, the possibility of which the popularity exceeds the threshold decreases. Thus, the minimum size of a swarm invading the tidal pool increases.

Because a swarm generated by our model is so robust that a swarm can go through the tidal pool once the swarm enters

the water. Yet, if an agent is isolated in the water, then he or she cannot move and is left alone. This phenomenon is also observed in real solider crabs.

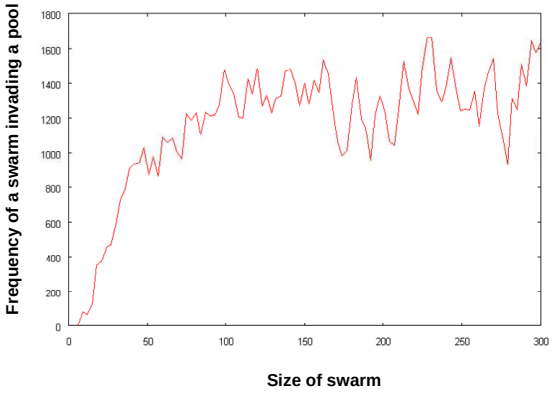

Figure 4 Frequency of a swarm invading a tidal pool as a function of swarm size.

Hourglass made of soldier crabs

In field observations, we found a soldier crab moving along the wall in a closed container, and we created an hourglass made of real soldier crabs (Nishiyama et al., 2011). Forty soldier crabs are collected and are confronted in a closed container, where the floor was made of cork providing friction enough to walk for soldier crabs. If the container is left for while, solder crabs walk along the wall in keeping a half-broken swarm. Since a concentrated swarm oscillates along the wall, the hourglass made of soldier crabs produced periodic oscillations for approximately two or three hours with a period of 70 seconds.

This behavior can be approximated by our model by slightly modifying one rule.

To simulate hourglass behavior as shown in Fig. 5 and 6, we introduced a tendency to walk along a wall. The hourglass scenario is constructed as follows. We first defined the wall state for any lattice (x, y) such that

$$w(x, y)=1 \text{ if the site is the wall state; } 0, \text{ otherwise.} \quad (9)$$

In the hourglass simulation, an agent can be located only at a site where $w(x, y) = 0$. The angle of tangential direction is defined for each wall state site (x, y) and is represented by $\theta_w(x, y)$. The tendency of walking along a wall is defined by

$$\theta_{k,t}=Rd\{\beta, \beta+\pi\} \quad (10)$$

$$\beta=Rd\{\theta_w(x, y)|d(\boldsymbol{P}(k, t), (x, y))\leq d(\boldsymbol{P}(k, t), (u, v)), w(x, y)=w(u, v)=1, (x, y), (u, v)\in N_W\}, \quad (11)$$

where $d((p, q), (x, y))$ represents the metric distance between two sites (p, q) and (x, y), and N_W represents the neighborhood of wall-monitoring for each agent. If an agent is close to the wall with respect to N_W, the agent's velocity, $\theta_{k,t}$ is parallel to the tangential direction of the wall. After this operation, velocity matching (equation (7)) is applied to all agents. Only from (10) and (11) can agents close to the wall walk along the wall and other agents pass using the shortcut.

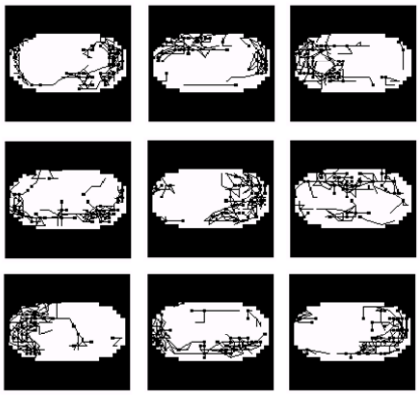

Figure 5 Snapshots of the time development of swarm move in the model simulation for the hourglass. Time proceeds from left to right and top to bottom. For this simulation, $P = 10$, $\alpha = 0.5$, $L = 4$, and $r_a = r_f = 2$. Each agent is represented by a black square with its own trajectory. First (top left) a main swarm is located at right hand, and then it moves to the left (top right). After that the swarm moves to the right again (middle center), and so on.

A solitary agent separated from a flockmate in our model undergoes a random walk because a potential transition is randomly chosen for each step. It follows that potential transitions stand for inherent noise. Whenever agents are highly concentrated, mutual anticipation can occur; inherent noise positively contributes to form a dense swarm. Thus, even if agents are exposed to large external perturbations, the perturbed transitions cannot be distinguished from inherent noise. A swarm resulting from mutual anticipation is thereby robust to external perturbation. In order to demonstrate the robustness of a swarm we implement "crab hour glass" (Nishiyama et al., 2011).

Fig. 5 shows snapshots of model simulations. It was assumed that an individual has a principal vector parallel to the tangent of the wall if it was close to the wall, in which the direction is chosen with uniform probability to be clockwise or anti-clockwise. Other rule settings were the same as in previous models. In the simulations, high concentrations initially occurred at the left or right ends, and the swarm rotated anti-clockwise. Most of the individuals walked along the wall, and some followed shortcuts. After a long period, the rotational direction reversed from clockwise to anti-clockwise and vice-versa.

The numbers of individuals in the divided areas (left, center, and right) shows regular oscillations (Fig. 6). The oscillating behavior of the model satisfies the properties of an hourglass of real soldier crabs. This oscillation mechanism is different from the periodic pattern of insect swarms based on escape-and-pursuit behavior.

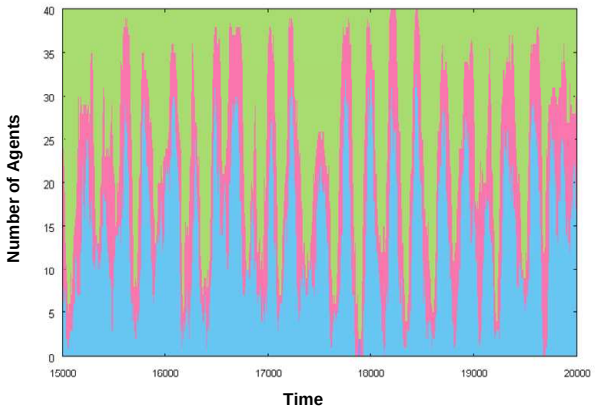

Figure 6 Numbers of agents in the left (blue), center (red) and right (green) areas of the container over time. For this simulation, $P = 10$, $\alpha = 0.5$, $L = 4$, and $r_a = r_f = 2$.

Logic gates made of soldier crabs

A swarm is so robust that it can be used as a ball for collision-computing (Adamatzky, 2002). In addition to the hourglass model, we prepared a special scenario in which the area in which agents can move freely is tightly bounded by a wall, and there is a gradient of preferred direction. The constructed OR gate made of agents is shown in Fig. 7.

Each diagram of Fig. 7 shows a snapshot of the behavior of OR gate in time. Two entrances on the left represent input positions for two variables x and y, and one exit on the right represents the output position for x OR y. If a swarm is present at position x, this state represents x=1. Agents move along the wall and rightward because of the gradient. After the collision of two swarms (each consists of 40 agents), the united swarm moves rightward and reaches the output position. It reveals x OR $y = 1$ for $(x, y) = (1, 1)$. Because x OR $y = 1$ for $(x, y) = (0, 1)$ or $(1, 0)$, and x OR $y = 0$ for $(x, y) = (0, 0)$, this setup can implement the OR gate.

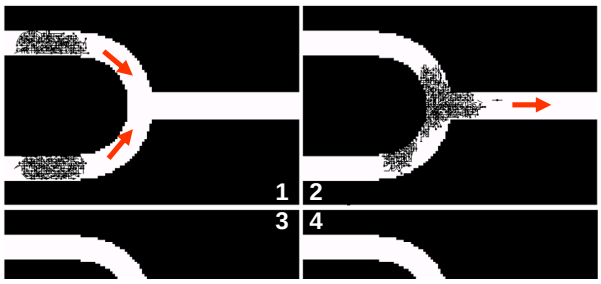

Figure 7 An OR gate of swarm balls. A swarm ball consists of 40 agents. Each agent is represented by a square with its 5-step trajectories. Four snapshots of a swarm at different time steps are numbered. Red arrows represent the direction of motion of a swarm ball.

AND and NOT gates were also constructed using a swarm. Fig. 8 shows the behavior of an AND gate. In each diagram, two entrances on the left represent x and y for input, and the three exits on the right represent x AND NOT(y), x AND y, and NOT(x) AND y, respectively. In the central exit on the right, there is a tidal pool in which a small swarm cannot enter. We define the tidal pool as a specific area U_p with the threshold $c = 10$. Because a swarm of 40 agents at the input position cannot enter the tidal pool, it retreats after the contact with the tidal pool and moves toward the output of x AND NOT(y).

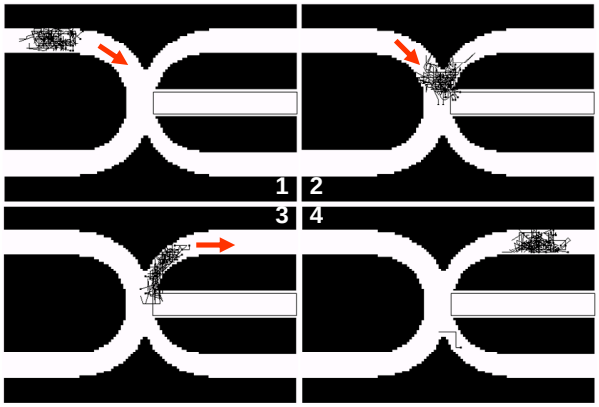

Figure 8 An AND gate of swarm balls. A swarm ball consists of 40 agents. Each agent is represented by a square with its 5-step trajectories. Four snapshots of a swarm at different time steps are numbered. Red arrows represent the direction of motion of a swarm ball.

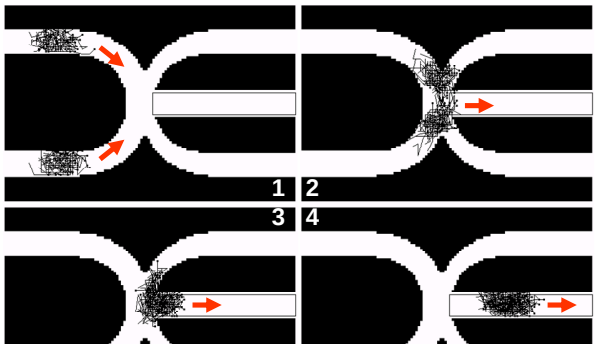

Figure 9 An AND gate of swarm balls. A swarm ball consists of 40 agents. Each agent is represented by a square with its 5-step trajectories. Four snapshots of a swarm at different time steps are numbered. Red arrows represent the direction of motion of a swarm ball.

Fig. 9 shows the behavior of an AND gate for $(x, y) = (1, 1)$. In this case, the collision of two swarms creates a large and united swarm, which enters the tidal pool. Thus, a united swarm produces the output of x AND y. If a swarm ball located at the input position of y is part of the logic gate, NOT(x) AND y can be utilized for NOT(x) for input x. Thus, this device can be utilized as a NOT gate. In this AND gate for $(x, y) = (1, 1)$ sometimes the united swarm does not enter the water pool. It results in low performance (72%).

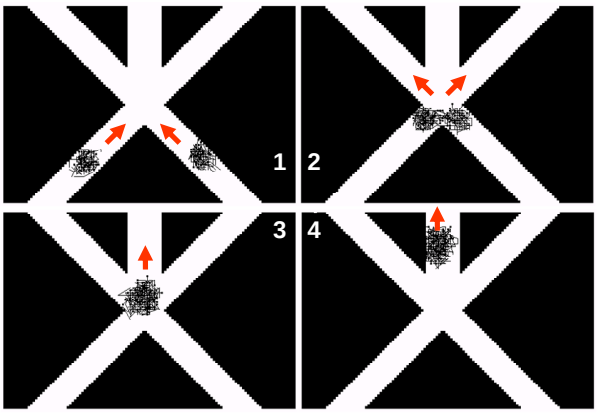

Figure 10 Another AND gate of swarm balls. A swarm ball consists of 40 agents. Each agent is represented by a square with its 5-step trajectories. Four snapshots of a swarm at different time steps are numbered. Red arrows represent the direction of motion of a swarm ball.

Thus we construct another AND gate as shown in Fig. 10. We set the initial principal directions of agents by the direction along the corridor represented by red arrows in the diagram 1 in Fig. 10. Actually we implement this gate by real soldier crabs. If the soldier crabs are set at the initial position and are threatened by a shadow suddenly appeared, they move straight. That is underlying implementation corresponding to the initial setting for principal vectors of agents. The swarms go straight. After the collision the united swarm moves following the united vectors. The performance of this AND gate is beyond 95%.

We here show three dynamics of our swarm model, water-crossing, hourglass and logic gate behaviors. The underlying mechanisms are based on mutual anticipation or inherent noise, which contribute to a robust, coherent swarm containing inherent turbulence. The characteristic flexibility and robustness of a swarm can be compared to a human's body awareness. A bird flock forms a large sub-domain that scales linearly with flock size. Because the proportion of the correlated domain against flock (body) size is constant, the flock appears to move as a single body (Cavagna et al., 2010). Our model can also show the scale-free correlation that has been observed in starlings and soldier crabs (Murakami et al., 2011). We believe that mutual anticipation is a key component in the generation and/or embedding of body awareness in a system. We now implement these logical gates by real soldier crabs, and the results will be given anywhere.

Robustness of a swarm plays an essential role in water-crossing, hourglass and logic gate behaviors. Because of robustness, a swarm can cross the water without being fallen into separated, hour glass shows periodic oscillation and logic gate shows high performance. In our model inherent noise (i.e. a number of potential transitions for each agent) contributes to make a robust swarm. Even if external perturbation is very large, the inherent noise cannot be distinguished from external perturbation. It entails that even external noise can coordinate to a robust swarm.

Even if the external noise increases, density and polarization of a swarm is not changed at all and a robust swarm is maintained, as shown in Fig. 11. The external perturbation is given by the product of the strength of a noise, λ and random variable, ξ. The random variable, ξ, is randomly chosen from [0, 1] and is coupled with velocity matching. When the projected velocity of agent is expressed as (v_x, v_y), $v_x + \lambda\xi$ and $v_y + \lambda\xi$ are given for the unit vector. In this simulation $P = 20$, $\alpha = 0.5$, $L = 4$, and $r_a = r_f = 2$. We tried other conditions with respect to P, and obtain similar results of polarization and density for $10<P<20$.

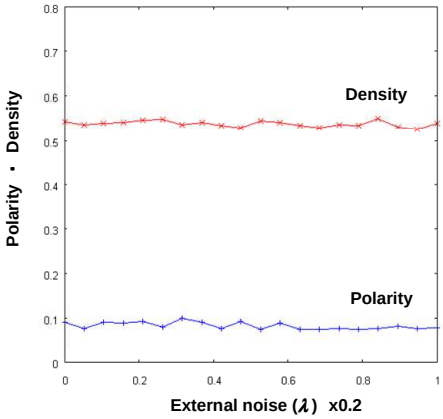

Figure 11. Polarization and density of a swarm generated by the model plotted against external noise.

In the next section, we discuss the significance of mutual anticipation to embodiment.

Future and Past coordinate Present

The question whether a swarm, flock or school has a single consciousness or body has been addressed by investigating kinetic data from real animal groups and model simulations. A notable finding is that a swarm or a flock has a scale-free proportion of correlated domains, which reveals embodied collective behavior. Although it has been suggested that the interplay between anticipated states and memory states can contribute to a scale-free correlation in an asynchronous updating model (Gunji et al., 2011), our model is the first attempt to implement the interplay of anticipated and memory states in a swarm. We here discuss the relationships among the concept of body awareness, the interplay of anticipated and memory states, and flexibility and robustness.

Body awareness is studied in terms of a sense of ownership (SoO) and of a sense of agency (SoA) in neuroscience. It is known that SoO and/or SoA can be easily implanted in an object instead of a participant's own body through a synchronous interplay of visual and tactile stimuli (Ramachandran et al., 1996, 1998) .

The generation of SoO and SoA in cognitive systems has also been studied. Fig. 10a shows a schematic diagram of SoO and SoA in sensory-motor coupling (Pfeifer, et al., 2007, Gallagher, 2000, Synofzik, 2008). After receiving a stimulus from the environment, a controller (brain) computes the anticipated state of its motor to adapt itself to the environment. The order from the controller is sent to the motor, and the actual state is revealed. A reaction from the environment is received again. In this scheme, the anticipated state processed on motor command is compared to the original intention in a controller. Because the comparison between the anticipated state and the original intention is executed before the motor moves, it constitutes a feed-forward process. In contrast, the actual state of the motor is compared to the original intention after the movement of the motor. This dynamic constitutes feed-back process. SoA is thought to be related to a feed-forward and SoO to a feed-back process (Gallagher, 2000).

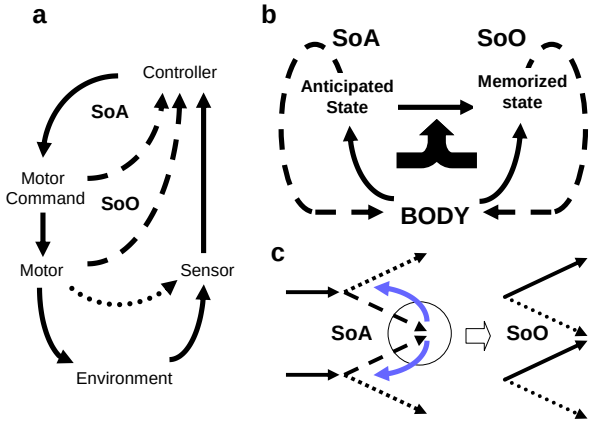

Figure 12. Sense of ownership (SoO) and sense of agency (SoA) in embodiment compared with body awareness in a swarm model. (a) Schematic diagram of SoO and SoA in a sensory-motor coupling system. (b) The schematic diagram of SoO and SoA in a system in which the sensory-motor distinction is vague in the "embodied body". (c) SoA and SoO in our swarm model. Blue arrows represent back propagation in time from the anticipated popularity of transitions.

Because adaptive cooperation in a system entails the exploitation of decentralization and embodiment, the body includes redundancy resulting from reciprocal conflicts among components (Cruse et al., 2006). Such redundancy makes it possible to achieve complementary interplay between different modalities without forced learning and can result in a vague distinction between body and environment (Lungarella at al., 2006). The body and/or the boundary between the body and the environment is perpetually generated and maintained. The scheme involving SoO and SoA when the environment, sensor and controller are mixed up in the form of body is represented in Fig. 12b. The motor command and motor are here represented by their featured, anticipated and memory states. In Fig. 12a, SoO and SoA constitute a hierarchical system. However, if there many redundant paths from controller to motor and embodiment between parts of the system can occur (i.e. the boundary of subsystems in a sensory-motor system becomes indefinite), the relationship between SoO and SoA in Fig. 12a can be replaced by that in Fig. 12b in which SoO and SoA are distributed in a parallel manner (Gunji, Sonoda & Niizato, 2011). The connection between SoO and SoA is dynamically generated to ensure consistency.

The dynamical connection between SoA and SoO is embedded in our swarm model. Through mutual anticipation, the anticipated popular sites are propagated backward in time, which can reveal actual transitions by asynchronous updating. Due to asynchronous updating and the avoidance of collisions by agents, a swarm is perpetually generated as a coherent system. These features can give rise to dynamic, flexible and robust swarming. After that, actual transition is memorized and is utilized as a principal vector to generate inherent noise (i.e., potential transitions) along the principal vector. SoO is here implemented as a reservoir to generate inherent noise or potentiality.

The underlying mechanisms of SoO and SoA emerge clearly in our swarm model. The interplay of anticipation and memory plays a central role in flexible and robust swarming. This interplay is characteristic of body awareness. Because a swarm is generated as a "body", it can show a coherent density containing inherent turbulence. The swarm is robust to perturbed environments. A system that appears to be in equilibrium (e.g., a swarm ball or hourglass showing periodic oscillations) is in fact perpetually and robustly generated far from equilibrium. The idea of a "body" is thus well-defined not in the context of stability but of robustness.

Conclusion

Based on the field observations of soldier crabs, *Mictyris guinotae*, we find that inherent noise can contribute to a dynamic and coherent swarm in which internal turbulence continuously flows. We implement such a phenomenon by an aggregation of agents of which each one have multiple potential transitions and can anticipate with each other. As a result we obtain dynamic and robust swarm even against the external perturbation.

Due to the robustness the swarm cannot be disturbed in perturbed environments such as water pool, and can be utilized as hour glass and logic gate. They are preliminary implemented by real soldier crabs, and that can be approximated by our model.

Since the swarm model is equipped with anticipation and memory, the model can be compared to the comparator model for SoA and SoO in body image, as long as a hierarchical structure is given up. Two loops including anticipated state or past state (memory) can cooperated with generating the current state. This structure is an essential structure to generate human body image. Our argument entails that a

swarm structure in our model can have a similar structure. Actually in the swarm a part of the swarm can be moved and operated by the swarm itself (corresponding to SoA). It results in a coherent and robust swarm as a whole not to be fallen into collapse of the swarm. This is the first step to connect the swarm with body image with respect to inherent time structure.

References

Adamatzky, A. Collision-based computing, Springer, 2002.

Ballerini, M., Cabibbo, V., Candelier, R., Cisbani, E., Giardina, I., Lecomte, V., Orlamdi, A., Parisi, G.P.A., Viale, M. and Zdravkovic, V. (2008a) Empirical investigation of starling flocks: A benchmark study in collective animal behavior. *Animal Behavior* 76: 201–215.

Ballerini, M., Cabibbo, N., Candelier, R., Cavagna, A., Cisbani, E., Giardina, I., Lecomte, V., Orlandi, A., Parisi, G., Procaccini, A., Viale, M., and Zdravkovic., V. (2008b) Interaction ruling animal collective behavior depends on topological rather than metric distance: Evidence from a field study. *PNAS* 105: 1232-1237.

Botvinick, M. and Cohen, J. (1998) Rubber hands 'feel' touch that eyes see. *Nature* 391: 756.

Bradshaw, C. and Scoffin, T.P. (1999) Factors limiting distribution and activity patterns of the soldier crab Dotilla myctiroides in Phuket, South Thailand, *Mar Biol* 135: 83-87.

Carere, C., Montanino, S., Moreschini, F., Zoratto, F., Chiarotti, F., Santucci, D., & Alleva, E. (2009) Aerial flocking patterns of wintering starlings, *Sturnus vulgaris*, under different predation risk. *Animal Behaviour* 77: 101-107.

Cavagna, A., Cimarelli, C., Giardina, I., Parisi, G.S.R., Stefanini, F. and Viale, M. (2010) Scale-free correlation in the bird flocks. *PNAS*, 107: 11865-11870.

Couzin, I.D. (2007) Collective minds. *Nature* 445: 715

Couzin, I.D.(2008) Collective cognition in animal groups. *Trends in Cog.Sc.*13: 36-43.

Cruse, H., Duerr, V. and Schmitz, J. (2007) Insect walking is based on a decentralised architecture revealing a simple and robust controller. *Philos. Trans. R. Soc. London* A 365: 221-250.

Czir´ok, A., E. Ben-Jacob, I. Cohen, and T. Vicsek (1996) Formation of complex bacterial colonies via self-generated vortices. *Phyl Rev* E 54 (2): 1791-1801.

Ehrsson, H.H., The experimental induction of out-of-body experience. *Science* **317**, 1048 (2007).

Gallagher, S. Philosophical conceptions of the self: Implications for cognitive science. *Trends Cognit. Sci.* **4**, 14–21(2000).

Gunji, Y-P., Niizato, T., Murakami, H., and Tani, I., (2010) Typ-Ken (an amalgam of type and token) drives Infosphere, *Knowledge, Technology and Policy* 23: 227-251.

Gunji, Y.-P., Shirakawa, T., Niizato, T., Yamachiyo, M. and Tani, I. (2011) An adaptive and robust biological network based on the vacant-particle transportation model. *J. theor. Biol.* 272: 187-200.

Gunji, Y-P., Sonoda, K. and Niizato, T. (2011) Embodiment and the paradox of the heap. *Radical Constructivism* (in press).

Lenggenhager, B., Tadi, T., Metzinger, T. & Blanke, O., Video ergo sum: manipulating bodily self-consciousness. *Science* **317**, 1096-1099 (2007).

Lungarella, L., Sporns, O., Mapping information flow in sensorimotor networks. *PLoS Comp. Biol*. **2**, 1301-1312. (2006).

Murakami, H., Niizato, and Gunji, Y-P., Scale-free proportion by the model based on potential resonance. *PLoS Comp Biol* (submitted).

Nishiyama, Y. Enomoto, K.., Toda, M., Gunji, Y.-P., Hour glass behavior of soldier crab, *Mictyris .guinotae*. 2011

Peter J. F., Hsi-Te Shih, D. and & Chan, B.K.K., (2010) A new species of *Mictyris guinotae* (Decapods, Brachyura, Mictiridae) from Ryukyu Island, Japan. *Crustaceana Monographs* 11: 83-105.

Pheifer, R. and Scheier, C., Understanding Intelligence. The MIT Press, Cambridge, 2001.

Pfeifer, R., Lungarella, M. and Iida, F., 2007, Self-organization, embodiment, and basically inspired robotics. *Science* **318**, 1088-1093.

Ramachandran, V.S., & Rogers-Ramachandran, D. Synaesthesia in phantom limbs induced with mirrors. *Phil. Trans. of the R. Soc. London. B, Biol. Sci.*, **263**(1369), 377–386 (1996).

Ramachandran, V. S., & Hirstein, W. The perception of phantom limbs. The D.O. Hebb lecture. *Brain*, 121, 1603–1630(1998)

Reynolds, C.W. (1987) Flocks, Herds, and Schools: A Distributed Behavioral Model. *Computer Graphics*. 21(4): 25-34.

Shih, J.T., (1995) Population-densities and annual activities of *Mictyris brevidactylus* (Stimpson, 1858) in the Tanshui mangrove swamp of northern Taiwan, *Zool. Stud.* 34: 96-105.

Sumpter, D.J.T., *Collective Animal Behavior*, Princeton, Univ. Press, Princeton, 2010.

Synofzik, M., Vosgerau, G. & Newen, G. Beyond the comparator model: A multifactorial two-step account of agency. *Consciousness and Cognition* **17**, 219–239 (2008)

Tsakiris, M., Prabhu, G. & Haggard, P. Having a body versus moving your body: how agency structures body-ownership. *Consciousness and Cognition* **15**, 423-432 (2006).

Varela, F.J., Evan, T. and Rosch, E., The Embodied Mind: Cognitive Science and Human Experience. Cambridge, MA: The MIT Press, 1992.

Vicsek, Y., Czirok, A., Ben-Jacob, E. and Shochet, .(1995) Novel type of phase transition in a system of self-driven particles. *Phys Rev Let* 75: 1226-1229.

Vicsek, T., Fluctuations and Scaling in Biology. Odford Univ. Press, Oxford, 2001.

Vicsek, T. and Zafiris A., Collective motion. *Arxiv preprint arXiv:1010.5017, 2010 - arxiv.org*.

Yates, C. A., R. Erban, C. Escudero, I. D. Couzin, J. Buhl, I. G. Kevrekidis, P. K. Maini, and D. J. T. Sumpterh (2009) Inherent noise can facilitate coherence in collective swarm motion, *PNAS* 106: 5464-5469.